This is the accepted manuscript of the article, which has been published in *Journal of Virology*. 2019, 93(20), e01130-19. https://doi.org/10.1128/JVI.01130-19

Slow infection due to lowering amount of intact versus empty particles is a characteristic feature of Coxsackievirus B5, dictated by the structural proteins

Paula Turkki[1,2], Mira Laajala[1], Marie Stark[1], Helena Vandesande[3], Heidi Sallinen Dal-Maso[1], Sailee Shroff[1], Anna Sävneby[3], Ganna Galitska[1], A. Michael Lindberg[3], Varpu Marjomäki[1]

1. Department of Biological and Environmental Science Division of Cell and Molecular Biology / Nanoscience Center, University of Jyväskylä, Jyväskylä, Finland.
2. Faculty of Medicine and Life Sciences, BioMediTech, Tampere University, Finland
3. Department of Chemistry and Biomedical Sciences, Linnaeus University, Kalmar, Sweden

ABSTRACT

Enterovirus B species typically cause a rapid cytolytic infection leading to efficient release of progeny viruses. However, they are also capable of persistent infections in tissues, which are suggested to contribute to severe chronic states such as myocardial inflammation and type 1 diabetes. In order to understand the factors contributing to differential infection strategies, we constructed a chimera by combining the capsid proteins from a fast cytolysis causing echovirus 1 (EV1) with non-structural proteins from Coxsackievirus B5 (CVB5) showing persistent infection in RD cells. The results showed that the chimera behaved similar to the parental EV1 leading to efficient cytolysis in both permissive A549 and semi-permissive RD cells. In contrast to EV1 and chimera, CVB5 replicated slower in permissive cells and showed persistent infection in semi-permissive cells. However, there was no difference in the efficiency of uptake of CVB5 in A549 or RD cells in comparison to the chimera or EV1. CVB5 virus batches constantly contained significant amounts of empty capsids, also in comparison to its close relative CVB3. During successive passaging of batch containing only intact CVB5, increasing amounts of empty and decreasing amounts of infective capsids were produced. Our results demonstrate that the increased amounts of empty particles and lowering amounts of infective particles is dictated by the CVB5 structural proteins leading to slowing down the infection between passages. Furthermore, the key factor for persistent infection is the low amount of infective particles produced, not the high number of empty particles accumulating.

IMPORTANCE

Enteroviruses cause several severe diseases with lytic infections that lead to rapid cell death but also persistent infections that are more silent, and lead to chronic states. Our study compared a cytolytic echovirus 1 infection to persistent coxsackievirus B5 infection by making a chimera between the structural proteins of echovirus 1 and non-structural proteins of coxsackievirus B5. Coxsackievirus B5 infection was found to lead to production of high number of empty viruses (empty capsids), that do not contain genetic material and are unable to continue the infection. Coinciding with high number of empty capsids, also the amount of infective virions decreased. This characteristic property was not observed in the constructed chimeravirus, suggesting that structural proteins are in charge of these phenomena. These results shed light on the mechanisms that may cause persistent infections. Understanding events leading to efficient or inefficient infection are essential in understanding the virus caused pathologies.

INTRODUCTION

Human enteroviruses are a large group of disease causing pathogens belonging to the family of *Picornaviridae*. Enterovirus infections in man can result in different diseases, from mild flu-like diseases to more severe symptoms such as meningitis, myocarditis and paralysis.

The icosahedral viral capsid is formed from four capsid proteins, VP1 to VP4. VP1, VP2 and VP3 are partly exposed from the capsid while VP4 is an internal protein that becomes exposed during early entry events and A-particle formation. The single-stranded enterovirus RNA genome of positive polarity encodes for 11 proteins, seven non-structural and four structural proteins in a single open reading frame. Both 3' (ending with a poly A sequence) and 5' ends of the genome have non-translated regions which are functional in the replication process.

Enterovirus B species contain different serotypes and novel, only genetically characterized types, including established and well characterized serotypes Coxsackieviruses B3 (CVB3), B5 (CVB5) and echovirus-1 (EV1). All CVBs use CAR as a receptor for attachment and entry (1, 2) but CVB1, 3, 5 and 6 may also use the decay accelerating factor (DAF, CD55) for attachment at the cell surface (3, 4). CAR is a tight junction localized transmembrane protein that can be used for entry into the cell (5,

6). The CVB/CAR interactions are associated with changes in the virion morphology resulting in A-particle formation and the release of the viral genome. In CVB3 this phenomenon has been suggested to start already during receptor binding and virus can internalize either with or without the receptor, depending on the cell type (7-9). EV1, on the other hand, uses the collagen-binding integrin α2β1, which is abundantly expressed in many cell types. EV1 internalizes together with its receptor and introduces a novel entry pathway, distinct from the natural pathway for the integrin receptors. In contrast to CVB interactions with CAR, EV1 binding to its integrin does not lead to uncoating but rather, uncoating takes place in non-acidic multivesicular structures and the viral genome is then released into the cytoplasm (10-12).

First signs of cell death can be seen after 4h p.i. leading to cell death within 8h p.i. depending on the virus and host cell (14). Most often the infections lead to cytolysis in cell cultures but enteroviruses may also cause persistent infections (15-19). Persistent infections have been suggested to cause chronic states leading to serious consequences, such as promoting the onset of type I diabetes in the pancreas tissue (20). Therefore, it is important to understand the detailed mechanisms behind switching between cytolytic and persistent infections. Enteroviruses have several mechanisms to cause the host cell death and, similarly, the host cell has several mechanisms to combat the virus infection and cell death (21). The interplay between host and the virus defines the outcome of the infection. Viral non-structural proteins act via inducing the host-cell shut-down, inhibiting cap-dependent translation and activating caspases. Viral structural proteins VP1, VP2 and VP3 have also been shown to have cause apoptosis, either by caspase activation or by cleavage of the poly-ADP ribose polymerase (PARP) (14).

In this study, a chimera between EV1 and CVB5 was constructed using reverse genetics and to study the role of non-structural and capsid proteins in the infection kinetics. The results show that the P1 region, contrary to P2 and P3, determines the efficiency and outcome of an infection. In this experimental model, the P1 region, encoding the CVB5 structural proteins, contain specific characteristics that lead to low amounts of intact virions and high incidence of empty capsids, which then slowed down the progression and kinetics of the secondary infection. We further show that the empty particles themselves did not inhibit cell binding or infection but the actual number of infective particles had a direct effect on infection kinetics.

MATERIALS AND METHODS

Cells. Virus productions and infectivity determinations were done in green monkey kidney cells (GMK) and cell experiments were carried out in human rhabdomycosarcoma (RD) and human lung carcinoma cells (A549). All cell lines were obtained from the American Type Culture Collection (ATCC) and maintained in either Eagle's Minimum Essential Medium (MEM) or Dulbecco's Modified Eagle Medium (D-MEM, Gibco Life Technologies) containing 5 to 10 % of fetal bovine serum (FBS), GlutaMAX, and penicillin-streptomycin antibiotics which were obtained from Gibco, Life Technologies.

Antibodies and reagents. The following primary antibodies were used in the experiments: monoclonal anti dsRNA antibody (J2; English & Scientific Consulting Kft.), rabbit polyclonal antibody against EV1 (12), anti CVB5 (DAKO; Monoclonal Mouse, Anti-Enterovirus Clone 5-D8/1), CVB3 capsids were detected with CVA9 targeted rabbit polyclonal antibody (kind gift from Merja Roivainen, THL, Helsinki). Fluorescently conjugated goat secondary antibodies were purchased from Molecular Probes, Invitrogen.

Cloning of chimera construct. The origin of the CVB5 strain *Dalldorf* (CVB5D) and its infectious cDNA clone have been described elsewhere (22-24). This virus was used by Reagan et al. for adaptation to cytolytic infection in RD cells by massive MOI (multiplicity of infection). Normal MOI results in a persistent infection of RD cells (24). Previously a recombinant variant of the infectious cDNA clone was used to generate an ancestor for the circulating CVB5 strains in the world and as an efficient recombinant infectious cDNA clone where the P1 regions was replaced by other enterovirus B structural genes (24, 25) and upon transfection resulted in replicating chimera viruses. A plasmid, pCR Script SK+, was constructed using the infectious cDNA clone of CVB5 where the complete genome was derived from the CVB5 genome sequence and unique restriction enzyme recognition sites where introduced enabling replacement cloning of the P1 region as previously described (26). The P1 region comprised of EV 1 (Farouk strain) P1 sequence thus coding for EV1 VP1-VP4 structural proteins and the remaining part of the genome was derived from the CVB5 genome (EV1/CVB5cDNA aka chimera). A pSPORT plasmid was provided for positive control experiments. This cDNA clone contains a complete EV1 genome including the P1, P2, and P3 sequence coding for the EV1 structural genes and corresponding NSPs (kind gift from Jeff Bergelson). The plasmids were amplified using ampicillin selection in DH5 cells and purified using Qiagen mini-prep kit. Plasmid size and correct

insertion was confirmed with restriction enzyme digestion and gel electrophoresis. GMK cells were transfected with EV1cDNA and chimera using a Lipofectamine protocols, changing media after 6hr incubation at 37C. Transfected cells were passaged until GMK cells were observed to cause cytolysis. Cells were collected, freeze thawed three times cell debris was pelleted down. Supernatants were used for crude virus infection of fresh GMK cells following virus purification.

Virus stock production. After successful transfection of the plasmids and production of the crude virus extracts, GMK cells were infected with the crude virus stocks of EV1, chimera, CVB3 (*Nancy* strain from ATCC) and CVB5 for 24 h in 5-layer bottles, after which the cells were collected and lysed via three freeze-thaw cycles. Viruses were purified as described earlier (27). Sucrose gradient 5 - 20% was used for CVB3 and CVB5 and fractions from 12 to 21 were collected. A separate batch of CVB5 was purified using 5-20% sucrose gradient but only fractions from 14 to 21 were collected to avoid empty particles. Also, empty capsids from fractions 8-11 were collected separately. For EV1 and chimera sucrose gradient of 10-40 % were used and three fractions on basis of the A260 nm spectrophotometric data were collected. Finally, collected virus fractions were concentrated using ultracentrifugation. Virus infectivity was assessed by end-point dilution and concentration of the virus stock was determined by the measurement of absorbance at A260 nm.

Cell viability assay. Cell viability was determined with the aid of Cell Titer Glo –kit (promega). Briefly, substrate was added straight to cell media avoiding the possible loss of loosely attached cells. Two to three independent experiments with at least three replicate samples were performed in each case.

Production of radioactively labelled of EV1, Chimera and CVB5. GMK or A549 cells were cultured until sub-confluency in MEM or D-MEM supplemented with 10% FBS, 1% Glutamax and 1% penicillin/streptomycin antibiotics. Cells were infected with EV1, chimera and CVB5 in low methionine/cysteine medium supplemented with 1% dialyzed FBS and 1% Glutamax. The infection was allowed to proceed at + 37 °C for 3 h, after which the medium was changed into fresh low methionine/cysteine medium supplemented with 1% dialyzed FBS and 1% Glutamax containing 50 µCi/ml of radioactive Sulphur. The infection was allowed to proceed at + 37 °C for another 15 h or 21 h so that the total infection time was 18 h or 24 h, respectively. The cells were freeze-thawed three times, after which 100 mM Octyl β-D-glucopyranoside (Amresco) was added to isolate membrane bound virus particles. Cell debris was centrifuged with a microcentrifuge 5415 D

(Eppendorf) at 16,000 rpm for 5 min. Supernatant was collected and added on top of 5-20% linear sucrose gradients. The gradients were collected from the top into 500 µl fractions. An aliquot from each fraction was added with scintillation cocktail (Ultima Gold MV, Perkin Elmer) and the CPM of each fraction was measured with liquid scintillation analyzer (Tri-Carb 2910 TR, Perkin Elmer). The fraction CPM was normalized to the sum of the total CPM of the whole gradient.

Immunolabeling and microscopy. An immunolabeling experiment was carried out in cells grown on coverslips. Cells were fixed with 4% PFA for 20 min at RT. The cells were permeabilized with 0.2% Triton X-100 and then treated with primary antibodies. After primary antibody incubation the cells were washed extensively with PBS. Appropriate secondary was added to cells at RT and incubated for 30 min and finally, the cells were extensively washed with PBS and mounted with Prolong gold antifade reagent supplemented with 4=,6-diamidino-2- phenylindole (DAPI) (Molecular Probes, Life Technologies). Immunolabeled samples were imaged with an Olympus IX81 microscope with a FluoView-1000 confocal setup. In total, 400 to 600 cells were imaged to manually quantify the percentage of replication and capsid positive cells.

Gel electrophoresis. The protein compositions of the virus stocks were analyzed by using a 4 to 12% NuPAGE Bis-Tris gel (Novex, Life Technologies). The proteins were denatured with the gel sample buffer provided by the manufacturer (NuPAGE; Life Technologies) at 100°C before they were loaded onto the gel. The gel was stained with commassie stain including fixative.

Passage assay. A549 cells were cultured on 96-well plates close to confluency in D-MEM supplemented with 10% FBS, 1% Glutamax and 1% penicillin/streptomycin antibiotics. Cells were infected with MOI 500 of EV1, chimera, CVB5 and CVB3 and the viruses were diluted in D-MEM supplemented with 1% FBS and 1% glutamax. The infection was allowed to proceed at +37 °C for 2 h, after which the medium was changed into fresh D-MEM supplemented with 10% FBS and 1% glutamax. The infection was then allowed to proceed at +37 °C for another 16 h. Next, half of the culture medium was passaged to new A549 cells and infection was allowed to proceed at +37 °C for 2 h, after which the medium was changed. The infection was then again allowed to proceed for 16 h at +37 °C. After passaging, the cells were always stained with crystal violet containing stain (8.3 mM crystal violet, 45 mM $CaCl_2$, 10% ethanol, 18.5% formaline, and 35 mM Tris-Base) for 10 min, after which excess stain was washed with water. Finally, lysis buffer (47.5% EtOH; 35 mM sodium

citrate; 12.5 mM HCl) was added to dissolve the stained cells and the absorbance was measured at 570 nm with a Victor X4 2030 multilabel reader (PerkinElmer).

Infection in the presence of empty capsids. A549 cells were cultured on 96-well plate in D-MEM supplemented with 10% FBS, 1% glutamax and 1% penicillin/streptomycin antibiotics. Cells were infected with the intact particles of CVB5 with MOI 0.7, 6.5, 21, 43 or 65 corresponding to 0.07, 0.65, 2.1, 4.3 and 6.5 ng, respectively. The virus mixture also contained different amounts of CVB5 empty particles (1.5, 3, 6 or 9 ng). The infection was allowed to proceed in D-MEM supplemented with 1% FBS, 1% glutamax and 1% penicillin/streptomycin antibiotics at +37 °C for 20 h. Next, the cells were stained with crystal violet containing stain (8.3 mM crystal violet, 45 mM $CaCl_2$, 10% ethanol, 18.5% formaline, and 35 mM Tris-Base) for 10 min, after which excess stain was washed with water. Finally, lysis buffer (47.5% EtOH; 35 mM sodium citrate; 12.5 mM HCl) was added to dissolve the stained cells and the absorbance was measured at 570 nm with a Victor X4 2030 multilabel reader (PerkinElmer).

Titration using end point dilution assay. GMK cells were cultured on 96-well plate in MEM supplemented with 10% FBS, 1% glutamax and 1% penicillin/streptomycin antibiotics. Cells were infected with the purified viruses or supernatants derived from passage assay by preparing a dilution series in MEM supplemented with 1% FBS and 1% GlutaMAX. The infection was allowed to proceed at + 37 °C for three days, after which the cells were stained with crystal violet stain (8.3 mM crystal violet, 45 mM $CaCl_2$, 10% ethanol, 18.5% formalin, and 35 mM Tris base). The excess stain was washed with water, and the 50% tissue culture infective dose (TCID50) was calculated by comparing the number of infected and uninfected wells for eight or four replicates of the same virus concentration. The concentration at which half of the wells would be infected was extrapolated (TCID50). Finally, the TCID50 value was multiplied by 0.7 to obtain the PFU/ml value.

RT-qPCR. A549 or RD cells were infected with EV1, chimera or CVB5 with MOI 10 in D-MEM supplemented with 1% FBS and 1% glutamax. After 1 h, cells were washed with PBS, after which the infection was allowed to proceed in D-MEM supplemented with 1% FBS and 1% glutamax for 2, 8, 24 or 48 h. At the end, the cells were freeze-thawed three times and cell debris was pelleted down at full speed with table top centrifuge. Viral RNA from the supernatant was extracted according to the instructions of the manufacturer using QiAmp viral RNA Mini Kit (Qiagen). Reverse transcription was carried out for positive strand RNA using 1.2 µM antisense (5'-GAAACACGGACACCCAAAGTA)

primer, 20 U M-MLV reverse transcriptase (Promega), 4 U RNAsin ribonuclease inhibitor (Promega) and dNTPs (Promega). The generated cDNA copy of the RNA was applied to qRT – PCR amplification using the 7500 Real-Time PCR System (Applied Biosystems) with 7500 SDS analysis software. Each reaction contained 5 ul template, 1 X Power SYBR Green Master Mix (Applied Biosystems) and 0.75 uM of antisense (5'-GAAACACGGACACCCAAAGTA) and sense (5'-CGGCCCCTGAATGCGGCTAA) primers for a final volume of 20 ul. The thermocycling protocol was executed as follows: pre – amplification step (involving denaturation and DNA polymerase activation) at 95 °C for 10 min.; 10 cycles of 15 s. at 95 °C, 30 s. at 64 °C – 55 °C (following a touch – down of 1 °C per cycle), and 40 s. at 72 °C; 30 cycles of 15 s. at 95 °C, 30 s. at 55 °C, and 40 s. at 72 °C; and dissocation curve generation for 1 cycle of 15 s. at 95 °C, 1 min. at 60 °C, and 15 s. at 95 °C. Each reaction was run in triplicate.

RESULTS

Enterovirus chimera containing the structural proteins of EV1 and non-structural proteins of CVB5 leads to an efficient replication and cytolysis in GMK and A549 cells, with infection kinetics resembling EV1

By using a previously described backbone of the CVB5 genome infectious cDNA clone (Fig 1A), replicating CVB5 and EV1/CVB5 viruses were generated. In addition, EV1 viruses were generated by transfection of an infectious cDNA clone in GMK cells. EV1, CVB5 and the chimera viruses infected GMK cells with a rather similar kinetics and cytolysis was typically seen after first 24 h of infection. EV1 and chimera both lead to efficient production of progeny viruses showing high infectivity and high protein concentration of 440 µg/ml and 870 µg/ml, respectively (Fig. 1B). CVB5 preparations had almost two logs lower measured virus titers but, in contrast, a significantly higher protein amount in comparison to the produced virus titers (pfu) (Fig 1B). Next, SDS-PAGE analysis of purified virus stocks was conducted in order to verify the purity of the viruses (Fig 1C). Similar protein amounts of all the virus stocks showed two clear bands corresponding to sizes between 25-37 kDa of approximately the same amount, indicating that all stocks were pure from major protein contaminants and contained only the viral capsid proteins.

Virus infectivity and infection kinetics were then studied in more detail in both permissive A549 and semi-permissive RD cell lines. A549 cells contain abundant amounts of the virus receptors CAR, DAF and $\alpha 2\beta 1$ integrins on their cell surface indicating these cells should be permissive for all three

viruses. RD cells on the other hand have been reported to have none or very limited CAR expression with only subpopulations of cells expressing the CAR on their cell surface (28).

First, A549 cells were infected with equal protein amounts of virus stocks and cell viability was measured at 12h and 24 h p.i. (Fig 1D). EV1 and chimera lead to rapid cytolysis: by 12h p.i. only half of the cells were alive and at 24 h p.i. the complete cytolysis was observed. Cytolytic capacity of CVB5 was notably slower, with 70 % of cells still viable at 24 h p.i. showing that cell destruction was greatly delayed. However, at 72 h (data not shown), also CVB5 demonstrated complete cytolytic efficiency. We then set out to compare cell viability after using similar number (virus titers) of infective particles (Fig 1E). The results showed a similar trend as seen with infections with equal protein amounts, suggesting that CVB5 infection kinetics was delayed when compared to EV1 and chimera at 24 h p.i.

Since CVB5 is known to cause persistent infection in RD cells, our next aim was to characterize the chimera infection in these cells as well. RD cells were infected first with equal protein amounts of virus stocks and cell viability was determined at 12 h and 24 h p.i. The results showed that EV1 and chimera were as cytolytic in RD cells as in A549 cells; around half of the cells had died at 12h p.i. and almost entire cultures had been destroyed at 24 h p.i. (Fig 1F). On the contrary, at 24h, only one third of CVB5 infected cells had lysed and even when the infection was continued until 48 h p.i., cell viability remained the same (data not shown). Again, we performed another viability assay using the same number of infective particles (Fig 1G). This experiment showed that not even high amounts of infective virions were able to cause lytic CVB5 infection in RD cells. At 12 h there was slight decrease in cell viability, but at 24 h CVB5 treated RD cells were as viable as the control. In contrast, EV1 and chimera showed efficient cytolytic infection.

Altogether, the results suggested that the chimera, consisting of EV1 capsid proteins and CVB5 non-structural proteins, was highly infective and cytolytic in both A549 and RD cells, in contrast to CVB5, suggesting that the structural proteins are contributing to the switch to cytolytic infection.

CVB3 and CVB5 both show persistent carrier culture infection in RD cells whereas in permissive A549 cells CVB5 has significantly slower infection kinetics

In order to study the possible role of the entry receptor, we included CVB3 in our studies as previous studies has shown that both CVB3 and CVB5 use CAR and DAF. First, we monitored CVB3 and CVB5

infection in both A549 and RD cells. We monitored viability of cells that were infected with equal MOI of viruses until 96 h p.i.. In A549 cells both viruses lead to the destruction of the entire cell culture within 96 h confirming a lytic replication mode in permissive cells (Fig 2A). Although both viruses demonstrated cytolytic replication of the cells in the end, CVB5 was notably slower than CVB3. At 24 h p.i., almost all of the CVB3 infected cells had died, while around 60 % of the CVB5 infected cells were still viable. Infected RD cell cultures did not show apparent cell lysis with either of the viruses (Fig 2C). Confocal microscopy confirmed the presence of viral capsid protein in minority of the cells in the culture during the 96 h time series (data not shown), suggesting that both viruses caused persistent infection in these cells. Even after 9 days of incubation with the viruses, no significant cytotoxicity was observed for the cell culture (data not shown). Since CVB5 infection was notably slower in A549 when compared to CVB3 when using the same MOI, similar to what was observed with EV1 and chimera (Fig 1B), we next studied in more detail the kinetics of capsid and dsRNA production. We infected A549 and RD cells with equal MOI, fixed the cells at different timepoints, immunolabelled against dsRNA and virus capsids and imaged with confocal microscopy. After imaging, we quantified the images in order to determine the presence of capsid positive cells (Fig 2B and D). In A549 cells, there was a clear difference in the percentage of dsRNA positive cells when CVB3 and CVB5 infections were compared. At 6 h p.i, about 35 % of infected cells showed positive label for dsRNA during CVB3 infections, whereas only 10% of CVB5 infected cells were positive at same timepoint. However, at 12h both infections were showing equal amount of dsRNA positive cells. As the same experiment was performed with RD cells (Fig 2D), there was no major difference in the number of cells showing infection between the two viruses for the first 48 h; viruses could only replicate in a small subpopulation of cells. Cells infected with either of the virus showed only around 10 % of the population that had newly synthetized capsid proteins present until 48 h p.i.

To conclude, these results suggested that both, CVB3 and CVB5, eventually lead to cytolytic infection in A549 cells and persistent infection of the RD cells but, importantly, CVB5 infection kinetics is slower than CVB3.

CVB5 batches produced in GMK cells contain high-amounts of empty capsids

As CVB5 was notably slower in A549 cells, we started to compare the CVB3 and CVB5 virus stocks in detail. First, as we compared the pfu/ml to mg/ml status of CVB3 and CVB5, we noticed a similar

phenomenon as when compared to EV1 and Chimera (Fig 1B): CVB5 contained more protein in relation to its pfu/ml when compared to CVB3 (Fig 3A). For more detailed understanding of the status of the viruses in purified batches, we performed transmission electron microscopy (TEM) analysis of the virus stocks (Fig 3B). Negatively stained TEM samples showed that EV1 and chimera mostly contained infectious virions (N-form), intact particles showing as light-coloured particles in TEM images. Only a small percentage of empty, dark labeled particles were observed per frame. In contrast, CVB5 batches had approximately 40 % of the virus particles with dark interior, suggesting that the batch contained significant portion of empty capsids. This was an interesting finding and possibly an explanation for differences observed during infection between these viruses.

Furthermore, when purified batches of CVB3 and CVB5 were compared, TEM analysis showed that CVB5 batch consisted of only approximately 50 % intact particles, whereas CVB3 batch contained mostly intact particles (Fig 3B, bottom row). Altogether, these results showed that CVB5 batches systematically contained high proportions of empty particles further explaining high virus protein concentration vs infectivity readings.

Purified batch of CVB5 containing only intact particles leads to efficient infection

We then continued to further elucidate the role of the empty particles with CVB5 that only contained complete virions, N particles. The intact viruses (160 S form of the virus) were separated from the empty virions and isolated from the bottom part of the 5-20% sucrose gradient. TEM analysis using negative staining confirmed that the new virus batch contained only intact virions (Fig 4A). Gradient fractionation of metabolically labeled viruses revealed no major differences between the various viruses in GMK cells and suggested that all of them contained a majority of N particles and a rather similar low amount of empty virions (Fig 4B). Similar results were obtained with A549 cells (Fig 4B). Also, cell viability measurement in A549 and RD cells after infection for 24 h, with the same amount of intact virus, showed that CVB5 infection was almost as efficient in infection in comparison to EV1, chimera and CVB3 in A549 cells and non-cytolytic in RD cells (Fig 4C). In order to look at the replication kinetics in more detail, we decided to compare the amount of replication using qPCR of the (+) strand RNA after using similar amount of infective particles from different constructs in A549 cells. The results showed that the amount of virus load taken up during 2 h is very similar between EV1 and chimera (Fig. 4D). Interestingly the, amount of CVB5 taken up during 2 h was even higher. There was no difference between the amounts of RNA produced after 8, 24 or

48 h. This result was replicated in an immunolabelling analysis detecting the replication intermediate dsRNA and capsid by confocal microscopy (Fig 4E): EV1, chimera and CVB5 (intact) showed ample amount of dsRNA and capsid in A549 cells.

qPCR evaluation of CVB5 replication in RD cells showed also that the uptake during 2 h to RD cells was as efficient as with other constructs (Fig 4D). However, there was a clear difference after 8 h in the amount of RNA produced: the amount of RNA was significantly lower, and the lower amounts were also evident after 24 and 48 hours.

Generation of empty capsids during CVB5 replication is a characteristic trait that shows up during serial passaging but do not explain the silencing of the infection

We then wanted to see how the infection would proceed within next generations when using the CVB5 batch that only had intact particles. A549 cells were infected with equal MOIand the infection efficiency as CPE was monitored during several passages until passage 4 (Fig 5A). Crystal violet staining of the passaged plates revealed that the first overnight infection by all viruses readily lifted the cells from the wells indicative of good infection. However, when we dissolved the crystal violet color and quantified the signal, the results showed that already during this first CPE, CVB5 showed lower amount of detached cells in comparison to other viruses. The next passages showed a much clearer difference between CVB5 and other viruses, suggesting that almost all cells survived the CVB5 infection. In contrast, there was no significant difference between EV1, chimera and CVB3, all of them showing high CPE in all passages.

As the lower CPE for CVB5 could result either from higher number of empty or lower number of infective particles, we measured the amounts of infectious virus particles produced in each step from different constructs. The results showed that the EV1, chimera and CVB3 all had high amounts of viruses in all passages although the actual pfu/ml varied in between 10^6 and 10^7 particles (Fig 6B). Strikingly, quantification of the virions from CVB5 showed low pfu/ml of only 10^5 in the first passage, and from there on the titers were too low to determine titer measurements. The titers for CVB5 kept under detection level during all consecutive passages suggesting that the infectivity dropped very soon to a low level.

In order to study if the presence of empty particles could affect the CPE in A549 cells, we performed two different experiments: 1) First we used a similar amount of intact CVB5 particles, on top of

which we added increasing amounts of empty particles. This approach showed that the increasing amounts of empty capsids, the highest exceeding the number of intact virions by about 1.4 fold, did not affect the infectivity of CVB5. 2) Next, we used increasing amounts of intact CVB5 virions on top of which we added a similar and high amount of empty particles (Fig. 5C). Also this approach revealed only minor changes in cell viability, suggesting that at least the amounts of empty virions used in the assay did not harm CVB5 infection efficiency.

Altogether, these results show that CVB5 batches have a tendency to produce lower amount of intact particles and increased amounts of empty virus particles. The presence of empty capsids does not affect infectivity, whereas the lowering amount of infective particles lead to slower infection kinetics of permissive A549 cells.

DISCUSSION

Chimeric enteroviruses as an experimental approach has been an informative tool in studying different enteroviral traits. Recently, a chimeric CVB3 strain with 5' NTR of poliovirus was found to lead to less efficient replication than the parental strain. This was found to promote immunity against CVB3-mediated heart and pancreatic diseases, suggesting that chimeric viruses are useful in vaccine research (29). Another study with chimeric constructs between respiratory (EV-D68) and an enteric (EV-D94) EV, suggested that tropism was dictated by the capsid proteins, while innate immunity was transferred via the NS-proteins, providing information on the roles of capsid and NS-proteins (30). In general, the enterovirus type is determined by its P1 region. Due to high extent of sequence conservation in the P2 and P3 regions, this part of the genome may be regarded as a supportive and replicative backbone to the type determining P1 region. Recombination takes place in the nature and e.g. different chimeric variants between endogenous viruses and vaccine strains appear time to time (31). Also, our results showed that viral structural elements between members of the enterovirus B species are easily interchangeable within the EV-B group.

Our goal here was to see if chimeric enterovirus could reveal new information regarding the mechanisms of persistent infections and the efficiency of lytic replication. We constructed a chimera consisting of EV1 structural proteins and CVB5 non-structural proteins. These parental viruses were selected for their known differences in their infection kinetics in cell culture. EV1 is a fast-acting cytolytic virus, whereas CVB5 has been shown to lead to slower infection, when using the CVB5 strain and the cell types studied. The results altogether showed that the chimera was functional,

leading to fast cytolysis in A549 cells, highly resembling the EV1 infection kinetics. In contrast, CVB5 led to significantly slower onset of replication and CPE in A549 cells.

In cell cultures, enteroviruses usually cause lytic infections resulting in cell death from 6 h p.i. onwards. One exception to this rule seem to be the human rhabdomyosarcoma cell line (RD), which has been shown to result in persistent infection when infected with CVB2O (32), CVB3 (28) and CVB5 (16), whereas in Hela and A549 cells, these viruses cause cytolytic infection (data not shown). One hypothesis for this phenomenon has been low or negligible transient expression of CAR in RD cells (28). It is believed that the low CAR expression helps the virus to sustain a carrier culture persistency in RD cell cultures as only subpopulation of the cells can get infected. Our data here supports this hypothesis, as only subpopulation of the cells got infected and clear signs of cytotoxicity and cytolysis was observed in those infected cells (data not shown), but the cell culture in general kept viable. In addition to persistent infections, it seems that enteroviruses cultured in RD cells obtain adaptations that lead to increased CPE within the culture, and eventually to total cytolysis of the culture (26, 33). After nine passages of CVB2 Ohio-strain (CVB2O) in RD cells Polacek et al (32) reported a phenotype of CVB2O that caused cytolysis of the culture. Both the parental and the adapted strains lead to similar titers of cytolytic viruses in Hela cells, while parental strain was showing decreased replication level in RD cells. Cytolytic trait was identified to be due to single amino acid change within the exposed region of VP1 capsid protein (26), suggesting a role in receptor usage. By using a high MOI, it was however possible to adapt the persistent CVB2O infection to a cytolytic one and the single mutation needed was a single mutation in VP1 (26). CVB3 has also been previously shown to adapt to RD cells by serial passaging causing increased CPE in these cells. The obtained CVB3-RD strain had increased affinity to bind DAF in comparison to the prototype strain CVB3-Nancy (23). This ability has been later mapped to two amino acid changes in the VP2 capsid protein (34). Although both DAF and CAR mediate tight binding of the CVB3-RD particle, only CAR supports the A-particle formation and internalization of the virus, while DAF most likely has a sequestering role on the cell surface (35). In addition to receptor usage, even closely related viruses can promote differential antiviral effects in their host cell. For example, two viruses that are known to cause hand-foot-and-mouth disease (HFMD), EV71 and CVA16, lead to differential activation of the interferon response in RD cells, further reflecting to their infection efficiency (36).

Our studies on EV1, chimera and CVB5, demonstrated that chimera had similar characteristics to EV1 with respect to virus infection kinetics. Chimera showed efficient production of infective virus

particles, efficient replication as judged by qPCR and cytolysis with a similar time scale as with parental EV1. As CVB5 showed negligible cytolysis in RD cells, the results demonstrate that the 5´UTR or the non-structural P2-P3 part of the genome does not dictate the differences between the chimera/EV1 and CVB5. Altogether these results suggested that the differences between CVB5 and EV1/chimera rely on the structural proteins comprising the viral capsid. This led us to consider if receptor binding and entry pathway could explain the marked difference between the constructs. In order to compare CVB5 to another CVB with abilities to bind to same receptors, CAR and DAF, we chose to use CVB3 in our experiments. Despite these similarities, there was still a clear difference between these viruses, CVB3 being more cytolytic and efficient than CVB5 in permissive A549 cells, suggesting that other factors than actual receptor binding would contribute to the slower lysing of the cells during CVB5 infection. Furthermore, qPCR analysis of the uptake efficiency showed no difference between the viruses. We therefore started to look for other differences between these viruses.

The high number of empty virions in the CVB5 virus batches seemed to be the most apparent difference between the two CVBVs. This was proven by TEM and by careful characterization of protein and infective particle content of the preparations. Strikingly, the infection efficiency of the CVB5 batch containing only intact and infective full viruses did not differ much between the viruses during the first round of infection. The presence of empty capsid thus seemed to be a likely explanation to the reduced efficiency of infection in subsequent passages. However, detailed analysis of the role of empty viruses, by adding various amounts of empty viruses on top of intact virions showed clearly that the accumulation of empty virions does not interfere with infection using the applied experimental set up. The results thus indicated that low amounts of intact viruses produced and not the high amounts of empty viruses is the determining factor for the slowing down of infection. Why does this then occur? If we start with fully infective particles, the amount of infective particles drops in comparison to chimera and EV1 already after the first passage and is under the detection limit already during the second passage.

Empty capsids are typically produced in varying amounts among picornavirus infections. They sediment around 70 to 80 S in sucrose gradients and contain VP0, VP1 and VP3 (37-41), although there are reports of FMDV empty capsids that contain also mature VP2 and VP4 (42). One explanation for these procapsids is that they form a reservoir of capsids where the genome may possibly be inserted (38, 40). Despite empty capsids being common, there are also families of

picornaviruses, such as human parechoviruses and especially Ljungan virus, that have not been reported to produce empty particles (43). Ljungan virus shows substantial differences in the capsid structure indicating that a different capsid form could have an effect on the genome encapsidation and thus play a role in the production of empty particles (43).

There is some literature about the presence of defective infective particles (DIP) that naturally interfere infection and replication of many viruses, including hepatitis B and C, influenza A virus, Dengue virus, and poliovirus (44-47). DIPs show deletions of one or multiple genes and thus cannot replicate alone, but during co-infection with fully infective viruses, will interfere with the outcome of the virus infection (45). In our experiments, the TEM analysis and the metabolic labeling of CVB5 showed that our batches contained truly empty capsids without RNA content. Also, the fact that increasing amounts of CVB5 empty viruses did not interfere with intact virions, argue against DIPS present in our CVB5 population.

One possible reason for the observed low production of infective particles with CVB5 is to interfere with the virus assembly step in the cytoplasm. How could that be affected by the structural proteins, however, remains a puzzle. Could the assembly of new virions be disturbed during CVB5 infection? Altogether, our data here shows that capsid proteins are determining the efficiency of infection for the studied constructs, whereas 5´UTR and the non-structural proteins did not determine the switch between cytolytic and more silent infection in A549 and RD cells, respectively. CVB5 infection leads to production of lower amounts of infective virions in relation to high amount of empty virus particles, which delays the infection progress. If the empty capsids are removed, CVB5 infection will lead to more efficient CPE but will soon start getting slower again, suggesting that the production of empty particles in the expense of infective virions is a characteristic property of this CVB5 strain in these type of cells, a feature previously reported for several different enteroviruses. Furthermore, CVB5 behavior was different from CVB3, which uses the same cell surface receptors, further demonstrating that the slowing down may be more linked to affecting assembly rather than viral entry.

FIGURE LEGENDS

FIG 1. Production and characterization of EV1, chimera and CVB5 stocks in GMK cells. A) Schematic illustration of the chimera containing the P1 region from EV1 and P2 and P3, including the 5'UTR from CVB5. B) Graph showing the infectivity (pfu/ml) and protein concentration of the produced virus stocks. C) SDS-PAGE analysis of virus stocks. Each lane has 1 µg of virus. Graphs showing the cell viability of infected A549 cells (D and E) and RD cells (F and G) detected at 12h and 24h p.i.. In D and F, infections were done with equal protein concentration of 0,7 µg/ml, corresponding to MOI 500 of EV1 and chimera and MOI 9 of CVB5. In E and G, infections were done with MOI 500.

FIG 2. Characterization of CVB3 and CVB5 infection in A549 and RD cells. A) Cell viability measurements during different timepoints in A) A549 cells. B) Quantification showing the percentage of cells positive for capsid and dsRNA labelling in A549 cells. C) cell viability in RD cells D) IF labeling quantifications in RD cells. Cell viability assay Infections were done with MOI 65, with corresponding protein concentrations of 0,01 µg/ml for CVB3 and 1 µg/ml for CVB5. IF labeling quantifications were made from three independent experiments with three replicates in each of them (total of 750 to 1350 cells / sample). Infections were done with MOI 65, with corresponding protein concentrations of 0,01 µg/ml for CVB3 and 1 µg/ml for CVB5. Results are averages from four samples within one representative experiment with SEM. Statistical significances are marked with ** < 0,01, *** < 0,001, **** < 0,0001.

FIG 3. CVB5 produced empty virus capsids in GMK cells. A) Graph showing the infectivity (pfu/ml) and protein concentration of the CVB3 and CVB5 virus stocks produced in GMK cells. B) Structural characterization of the virus stocks with the aid of TEM images and negative staining with representative magnifications. Scale bar 200 nm.

FIG 4. CVB5 infection kinetics with batch containing only intact viruses A) TEM image of negative stained differentially produced CVB5 batch that mostly contained intact virus particles. B) Graph showing the cpm counts (% of total cpm) after virus infections of GMK or A549 cells performed in the presence of radioactive methionine/cysteine. Cells were infected with MOI 25. C) A549 or RD cells were infected with MOI 500 of EV1, chimera, CVB5 or CVB3 and cell viability (ATP) was determined at 24 h p.i.. D) RT-qPCR from EV1, chimera and CVB5 infected A549 and RD cells. The cells were infected with MOI 10, and after 1 h the medium was changed. The amount of positive sense RNA was determined from the lysed cells at 2,8,24 and 48 h p.i. cDNA of chimera was used as a positive control. E) Confocal images showing dsRNA and capsid distribution from A549 cells that were infected with EV1, chimera or CVB5, fixed and immunolabelled. 500 PFU/cell was first bound on ice for 1 h, after which excess virus was washed with 0.5% BSA in PBS. Infection was then allowed to proceed at +37 °C for 6 h.

FIG 5. The infection efficiency of CVB5 is decreased in next generations which is not due to disturbance of empty particles. A) Passage assay with CVB5 batch containing only intact particles at start. A549 cells were infected with EV1, Chimera, CVB5 and CVB3 and CPE was monitored for four generations by passaging a similar amount of culture supernatant to the next wells at 18 h intervals. Initial infection was done with MOI 500 for all constructs and the medium was changed after 2 h. B) PFU/ml values of supernatants from the passage assay in A, were determined with end-point dilution assay. C) CPE assay with intact CVB5 particles was carried out in the presence of increasing amount of CVB5 empty particles or increasing amount of intact particles (MOI 43 (4.3 ng), MOI 21 (2.1 ng), MOI 6.5 (0.65 ng), MOI 0.7 (0.07 ng)). Intact and empty particles were mixed together and added on A549 cells. The infection was allowed to proceed for 20 h, after which the cell viability was determined by crystal violet staining.

REFERENCES

1. Bergelson, J. M., J. A. Cunningham, G. Droguett, E. A. Kurt-Jones, A. Krithivas, J. S. Hong, M. S. Horwitz, R. L. Crowell, and R. W. Finberg. 1997. Isolation of a common receptor for Coxsackie B viruses and adenoviruses 2 and 5. Science. 275:1320-1323.

2. Martino, T. A., M. Petric, H. Weingartl, J. M. Bergelson, M. A. Opavsky, C. D. Richardson, J. F. Modlin, R. W. Finberg, K. C. Kain, N. Willis, C. J. Gauntt, and P. P. Liu. 2000. The coxsackie-adenovirus receptor (CAR) is used by reference strains and clinical isolates representing all six serotypes of coxsackievirus group B and by swine vesicular disease virus. Virology. 271:99-108. doi: 10.1006/viro.2000.0324 [doi].

3. Bergelson, J. M., J. G. Mohanty, R. L. Crowell, N. F. St John, D. M. Lublin, and R. W. Finberg. 1995. Coxsackievirus B3 adapted to growth in RD cells binds to decay-accelerating factor (CD55). J. Virol. 69:1903-1906.

4. Shafren, D. R., R. C. Bates, M. V. Agrez, R. L. Herd, G. F. Burns, and R. D. Barry. 1995. Coxsackieviruses B1, B3, and B5 use decay accelerating factor as a receptor for cell attachment. J. Virol. 69:3873-3877.

5. Bergelson, J. M., J. F. Modlin, W. Wieland-Alter, J. A. Cunningham, R. L. Crowell, and R. W. Finberg. 1997. Clinical coxsackievirus B isolates differ from laboratory strains in their interaction with two cell surface receptors. J. Infect. Dis. 175:697-700.

6. Cohen, C. J., J. T. Shieh, R. J. Pickles, T. Okegawa, J. T. Hsieh, and J. M. Bergelson. 2001. The coxsackievirus and adenovirus receptor is a transmembrane component of the tight junction. Proc. Natl. Acad. Sci. U. S. A. 98:15191-15196. doi: 10.1073/pnas.261452898 [doi].

7. Coyne, C. B., and J. M. Bergelson. 2005. CAR: a virus receptor within the tight junction. Adv. Drug Deliv. Rev. 57:869-882. doi: S0169-409X(05)00016-5 [pii].

8. Coyne, C. B., L. Shen, J. R. Turner, and J. M. Bergelson. 2007. Coxsackievirus entry across epithelial tight junctions requires occludin and the small GTPases Rab34 and Rab5. Cell. Host Microbe. 2:181-192. doi: S1931-3128(07)00163-1 [pii].

9. Delorme-Axford, E., Y. Sadovsky, and C. B. Coyne. 2013. Lipid raft- and SRC family kinase-dependent entry of coxsackievirus B into human placental trophoblasts. J. Virol. 87:8569-8581. doi: 10.1128/JVI.00708-13 [doi].

10. Karjalainen, M., N. Rintanen, M. Lehkonen, K. Kallio, A. Maki, K. Hellstrom, V. Siljamaki, P. Upla, and V. Marjomaki. 2011. Echovirus 1 infection depends on biogenesis of novel multivesicular bodies. Cell. Microbiol. 13:1975-1995. doi: 10.1111/j.1462-5822.2011.01685.x; 10.1111/j.1462-5822.2011.01685.x.

11. Rintanen, N., M. Karjalainen, J. Alanko, L. Paavolainen, A. Maki, L. Nissinen, M. Lehkonen, K. Kallio, R. H. Cheng, P. Upla, J. Ivaska, and V. Marjomaki. 2012. Calpains promote alpha2beta1

integrin turnover in nonrecycling integrin pathway. Mol. Biol. Cell. 23:448-463. doi: 10.1091/mbc.E11-06-0548.

12. Marjomaki, V., V. Pietiainen, H. Matilainen, P. Upla, J. Ivaska, L. Nissinen, H. Reunanen, P. Huttunen, T. Hyypia, and J. Heino. 2002. Internalization of echovirus 1 in caveolae. J. Virol. 76:1856-1865.

13. Marjomaki, V., P. Turkki, and M. Huttunen. 2015. Infectious Entry Pathway of Enterovirus B Species. Viruses. 7:6387-6399. doi: 10.3390/v7122945 [doi].

14. Buenz EJ, and Howe CL. 2006. Picornaviruses and cell death. Trends in Microbiology. 14:28-36. doi: https://doi.org/10.1016/j.tim.2005.11.003.

15. Chehadeh, W., J. Kerr-Conte, F. Pattou, G. Alm, J. Lefebvre, P. Wattre, and D. Hober. 2000. Persistent infection of human pancreatic islets by coxsackievirus B is associated with alpha interferon synthesis in beta cells. J. Virol. 74:10153-10164.

16. Argo, E., B. Gimenez, and P. Cash. 1992. Non-cytopathic infection of rhabdomyosarcoma cells by coxsackie B5 virus. Arch. Virol. 126:215-229.

17. Alidjinou, E. K., F. Sane, A. Bertin, D. Caloone, and D. Hober. 2015. Persistent infection of human pancreatic cells with Coxsackievirus B4 is cured by fluoxetine. Antiviral Res. 116:51-54. doi: 10.1016/j.antiviral.2015.01.010 [doi].

18. Engelmann, I., E. K. Alidjinou, A. Bertin, J. Bossu, C. Villenet, M. Figeac, F. Sane, and D. Hober. 2017. Persistent coxsackievirus B4 infection induces microRNA dysregulation in human pancreatic cells. Cell Mol. Life Sci. . doi: 10.1007/s00018-017-2567-0 [doi].

19. Kim, K. S., S. Tracy, W. Tapprich, J. Bailey, C. K. Lee, K. Kim, W. H. Barry, and N. M. Chapman. 2005. 5'-Terminal deletions occur in coxsackievirus B3 during replication in murine hearts and cardiac myocyte cultures and correlate with encapsidation of negative-strand viral RNA. J. Virol. 79:7024-7041. doi: 79/11/7024 [pii].

20. Hyoty, H. 2016. Viruses in type 1 diabetes. Pediatr. Diabetes. 17 Suppl 22:56-64. doi: 10.1111/pedi.12370 [doi].

21. Harris, K. G., and C. B. Coyne. 2014. Death waits for no man--does it wait for a virus? How enteroviruses induce and control cell death. Cytokine Growth Factor Rev. 25:587-596. doi: 10.1016/j.cytogfr.2014.08.002 [doi].

22. CROWELL, R. L., and J. T. SYVERTON. 1961. The mammalian cell-virus relationship. VI. Sustained infection of HeLa cells by Coxsackie B3 virus and effect on superinfection. J. Exp. Med. 113:419-435.

23. Reagan, K. J., B. Goldberg, and R. L. Crowell. 1984. Altered receptor specificity of coxsackievirus B3 after growth in rhabdomyosarcoma cells. J. Virol. 49:635-640.

24. Gullberg, M., C. Tolf, N. Jonsson, M. N. Mulders, C. Savolainen-Kopra, T. Hovi, M. Van Ranst, P. Lemey, S. Hafenstein, and A. M. Lindberg. 2010. Characterization of a putative ancestor of coxsackievirus B5. J. Virol. 84:9695-9708. doi: 10.1128/JVI.00071-10 [doi].

25. Jonsson, N., A. Savneby, M. Gullberg, K. Evertsson, K. Klingel, and A. M. Lindberg. 2015. Efficient replication of recombinant Enterovirus B types, carrying different P1 genes in the coxsackievirus B5 replicative backbone. Virus Genes. 50:351-357. doi: 10.1007/s11262-015-1177-x [doi].

26. Gullberg, M., C. Tolf, N. Jonsson, C. Polacek, J. Precechtelova, M. Badurova, M. Sojka, C. Mohlin, S. Israelsson, K. Johansson, S. Bopegamage, S. Hafenstein, and A. M. Lindberg. 2010. A single coxsackievirus B2 capsid residue controls cytolysis and apoptosis in rhabdomyosarcoma cells. J. Virol. 84:5868-5879. doi: 10.1128/JVI.02383-09 [doi].

27. Myllynen, M., A. Kazmertsuk, and V. Marjomaki. 2016. A Novel Open and Infectious Form of Echovirus 1. J. Virol. 90:6759-6770. doi: 10.1128/JVI.00342-16 [doi].

28. Carson, S. D., K. S. Kim, S. J. Pirruccello, S. Tracy, and N. M. Chapman. 2007. Endogenous low-level expression of the coxsackievirus and adenovirus receptor enables coxsackievirus B3 infection of RD cells. J. Gen. Virol. 88:3031-3038. doi: 88/11/3031 [pii].

29. Chapman, N. M., A. Ragland, J. S. Leser, K. Hofling, S. Willian, B. L. Semler, and S. Tracy. 2000. A group B coxsackievirus/poliovirus 5' nontranslated region chimera can act as an attenuated vaccine strain in mice. J. Virol. 74:4047-4056.

30. Royston, L., M. Essaidi-Laziosi, F. J. Perez-Rodriguez, I. Piuz, J. Geiser, K. H. Krause, S. Huang, S. Constant, L. Kaiser, D. Garcin, and C. Tapparel. 2018. Viral chimeras decrypt the role of enterovirus capsid proteins in viral tropism, acid sensitivity and optimal growth temperature. PLoS Pathog. 14:e1006962. doi: 10.1371/journal.ppat.1006962 [doi].

31. Combelas, N., B. Holmblat, M. L. Joffret, F. Colbere-Garapin, and F. Delpeyroux. 2011. Recombination between poliovirus and coxsackie A viruses of species C: a model of viral genetic plasticity and emergence. Viruses. 3:1460-1484. doi: 10.3390/v3081460 [doi].

32. Polacek, C., J. O. Ekstrom, A. Lundgren, and A. M. Lindberg. 2005. Cytolytic replication of coxsackievirus B2 in CAR-deficient rhabdomyosarcoma cells. Virus Res. 113:107-115. doi: S0168-1702(05)00157-7 [pii].

33. Carson, S. D., N. M. Chapman, S. Hafenstein, and S. Tracy. 2011. Variations of coxsackievirus B3 capsid primary structure, ligands, and stability are selected for in a coxsackievirus and adenovirus receptor-limited environment. J. Virol. 85:3306-3314. doi: 10.1128/JVI.01827-10 [doi].

34. Lindberg, A. M., R. L. Crowell, R. Zell, R. Kandolf, and U. Pettersson. 1992. Mapping of the RD phenotype of the Nancy strain of coxsackievirus B3. Virus Res. 24:187-196.

35. Milstone, A. M., J. Petrella, M. D. Sanchez, M. Mahmud, J. C. Whitbeck, and J. M. Bergelson. 2005. Interaction with coxsackievirus and adenovirus receptor, but not with decay-accelerating

factor (DAF), induces A-particle formation in a DAF-binding coxsackievirus B3 isolate. J. Virol. 79:655-660. doi: 79/1/655 [pii].

36. Zhang W, Zhang L, Wu Z, and Tien P. 2014. Differential interferon pathway gene expression patterns in Rhabdomyosarcoma cells during Enterovirus 71 or Coxsackievirus A16 infection. Biochemical and Biophysical Research Communications. 447:550-555. doi: https://doi.org/10.1016/j.bbrc.2014.04.021.

37. Putnak, J. R., and B. A. Phillips. 1982. Poliovirus empty capsid morphogenesis: evidence for conformational differences between self- and extract-assembled empty capsids. J. Virol. 41:792-800.

38. Shingler, K. L., J. L. Yoder, M. S. Carnegie, R. E. Ashley, A. M. Makhov, J. F. Conway, and S. Hafenstein. 2013. The enterovirus 71 A-particle forms a gateway to allow genome release: a cryoEM study of picornavirus uncoating. PLoS Pathog. 9:e1003240. doi: 10.1371/journal.ppat.1003240 [doi].

39. Basavappa, R., R. Syed, O. Flore, J. P. Icenogle, D. J. Filman, and J. M. Hogle. 1994. Role and mechanism of the maturation cleavage of VP0 in poliovirus assembly: structure of the empty capsid assembly intermediate at 2.9 A resolution. Protein Sci. 3:1651-1669. doi: 10.1002/pro.5560031005 [doi].

40. Cifuente, J. O., H. Lee, J. D. Yoder, K. L. Shingler, M. S. Carnegie, J. L. Yoder, R. E. Ashley, A. M. Makhov, J. F. Conway, and S. Hafenstein. 2013. Structures of the procapsid and mature virion of enterovirus 71 strain 1095. J. Virol. 87:7637-7645. doi: 10.1128/JVI.03519-12 [doi].

41. Wang, X., J. Ren, Q. Gao, Z. Hu, Y. Sun, X. Li, D. J. Rowlands, W. Yin, J. Wang, D. I. Stuart, Z. Rao, and E. E. Fry. 2015. Hepatitis A virus and the origins of picornaviruses. Nature. 517:85-88. doi: 10.1038/nature13806 [doi].

42. Curry, S., E. Fry, W. Blakemore, R. Abu-Ghazaleh, T. Jackson, A. King, S. Lea, J. Newman, and D. Stuart. 1997. Dissecting the roles of VP0 cleavage and RNA packaging in picornavirus capsid stabilization: the structure of empty capsids of foot-and-mouth disease virus. J. Virol. 71:9743-9752.

43. Zhu, L., X. Wang, J. Ren, C. Porta, H. Wenham, J. O. Ekstrom, A. Panjwani, N. J. Knowles, A. Kotecha, C. A. Siebert, A. M. Lindberg, E. E. Fry, Z. Rao, T. J. Tuthill, and D. I. Stuart. 2015. Structure of Ljungan virus provides insight into genome packaging of this picornavirus. Nat. Commun. 6:8316. doi: 10.1038/ncomms9316 [doi].

44. Yuan, T. T., M. H. Lin, D. S. Chen, and C. Shih. 1998. A defective interference-like phenomenon of human hepatitis B virus in chronic carriers. J. Virol. 72:578-584.

45. Dimmock, N. J., and A. J. Easton. 2014. Defective interfering influenza virus RNAs: time to reevaluate their clinical potential as broad-spectrum antivirals? J. Virol. 88:5217-5227. doi: 10.1128/JVI.03193-13 [doi].

46. Li, D., W. B. Lott, K. Lowry, A. Jones, H. M. Thu, and J. Aaskov. 2011. Defective interfering viral particles in acute dengue infections. PLoS One. 6:e19447. doi: 10.1371/journal.pone.0019447 [doi].

47. Song, Y., A. V. Paul, and E. Wimmer. 2012. Evolution of poliovirus defective interfering particles expressing Gaussia luciferase. J. Virol. 86:1999-2010. doi: 10.1128/JVI.05871-11 [doi].

Figure 1

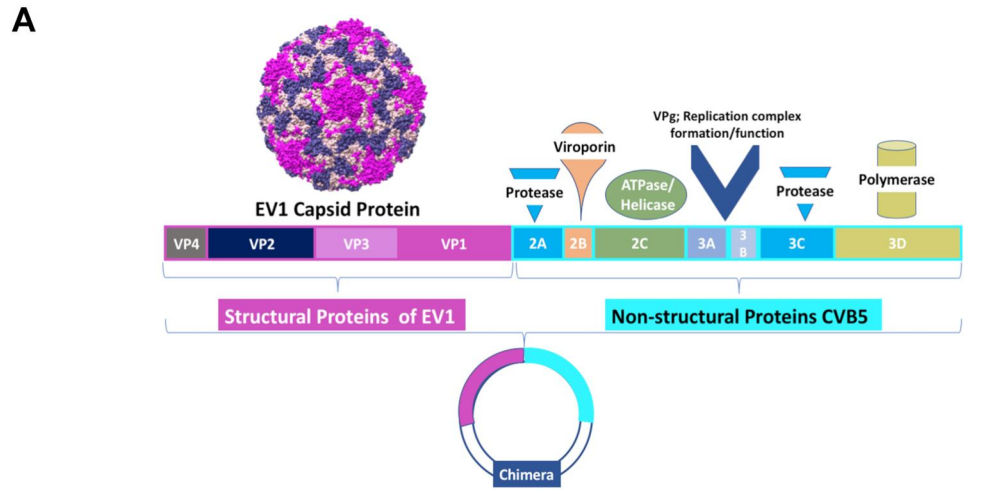
A
EV1 Capsid Protein
VP4
VP2
VP3
VP1
2A
2B
2C
3A
3B
3C
3D
Viroporin
Protease
ATPase/
Helicase
VPg; Replication complex
formation/function
Protease
Polymerase
Structural Proteins of EV1
Non-structural Proteins CVB5
Chimera

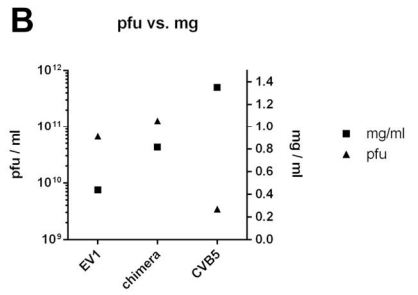
B
pfu vs. mg
pfu / ml
mg / ml
mg/ml
pfu
EV1
chimera
CVB5

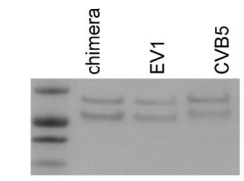
C
chimera
EV1
CVB5

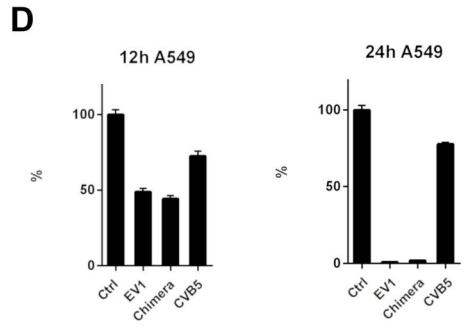
D
12h A549
24h A549
%
Ctrl
EV1
Chimera
CVB5

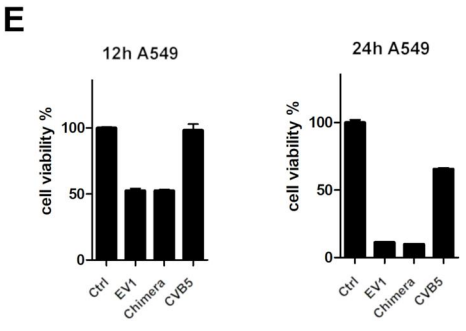
E
12h A549
24h A549
cell viability %
Ctrl
EV1
Chimera
CVB5

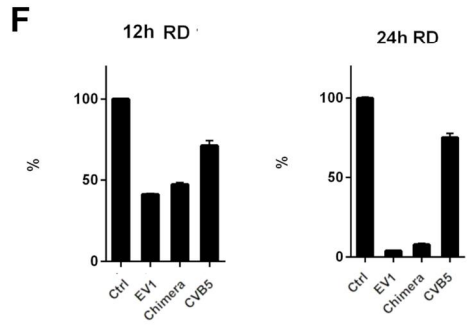
F
12h RD
24h RD
%
Ctrl
EV1
Chimera
CVB5

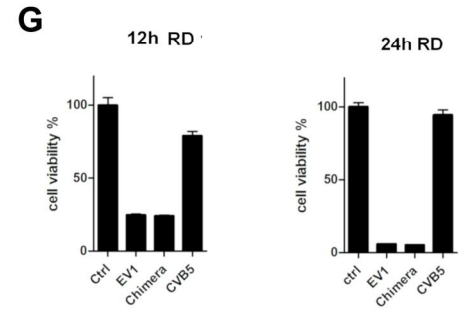
G
12h RD
24h RD
cell viability %
ctrl
EV1
Chimera
CVB5

Figure 2

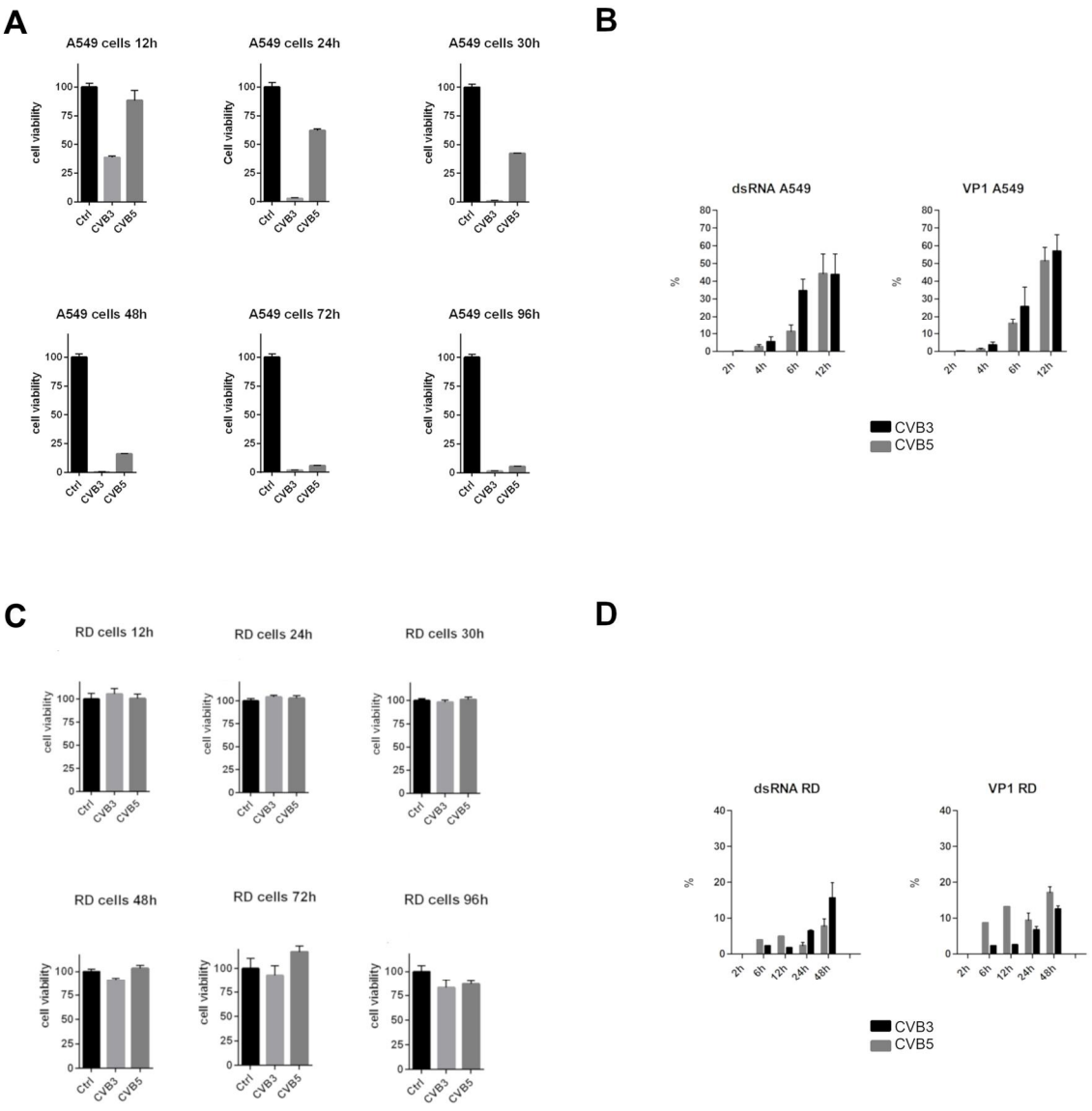
A
A549 cells 12h
A549 cells 24h
A549 cells 30h
A549 cells 48h
A549 cells 72h
A549 cells 96h
cell viability
Ctrl
CVB3
CVB5
B
dsRNA A549
VP1 A549
%
2h
4h
6h
12h
CVB3
CVB5
C
RD cells 12h
RD cells 24h
RD cells 30h
RD cells 48h
RD cells 72h
RD cells 96h
D
dsRNA RD
VP1 RD
2h
6h
12h
24h
48h

Figure 3

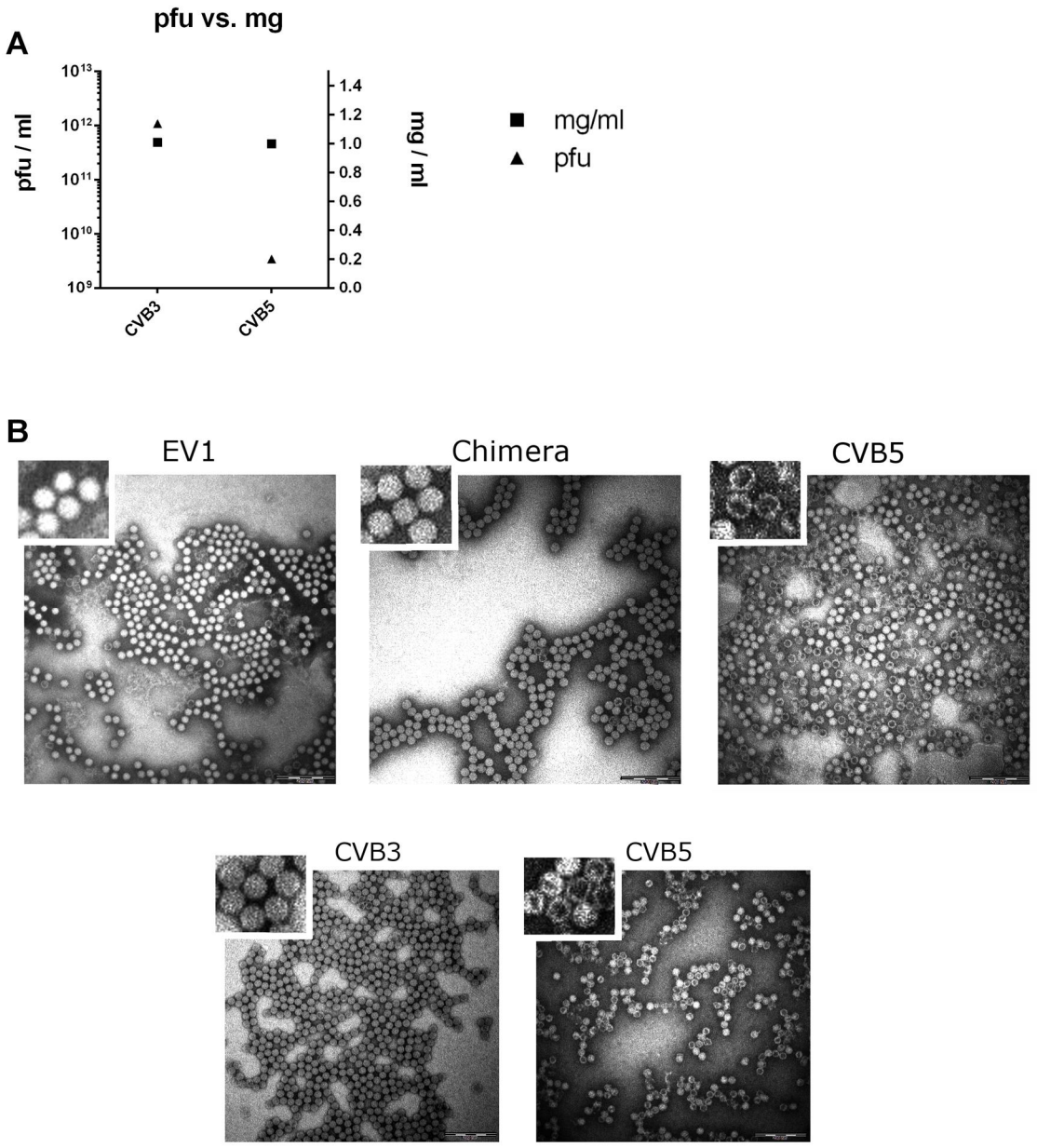
A
pfu vs. mg
pfu / ml
mg / ml
mg/ml
pfu
CVB3
CVB5
B
EV1
Chimera
CVB5
CVB3
CVB5

Figure 4

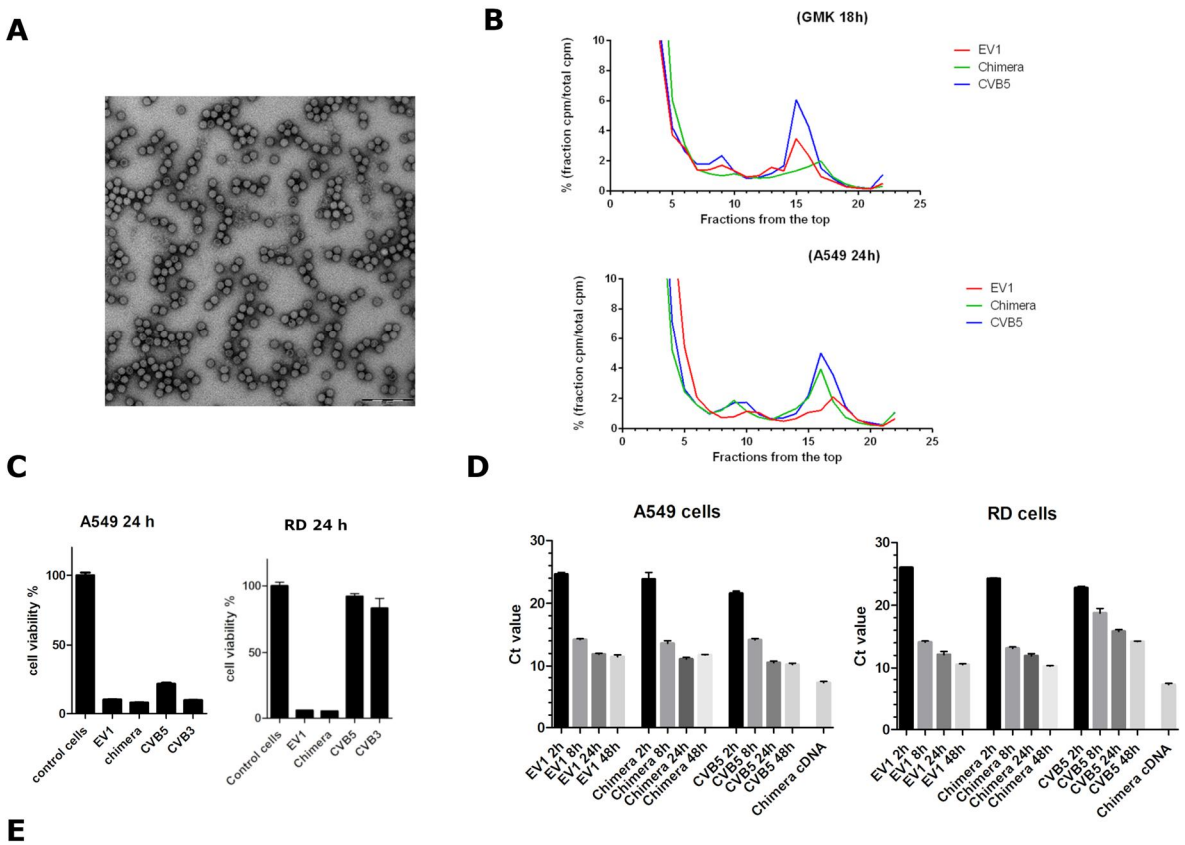
A
B
(GMK 18h)
EV1
Chimera
CVB5
% (fraction cpm/total cpm)
Fractions from the top
(A549 24h)
EV1
Chimera
CVB5
% (fraction cpm/total cpm)
Fractions from the top
C
A549 24 h
RD 24 h
cell viability %
control cells
EV1
chimera
CVB5
CVB3
cell viability %
Control cells
EV1
Chimera
CVB5
CVB3
D
A549 cells
RD cells
Ct value
EV1 2h
EV1 8h
EV1 24h
EV1 48h
Chimera 2h
Chimera 8h
Chimera 24h
Chimera 48h
CVB5 2h
CVB5 8h
CVB5 24h
CVB5 48h
Chimera cDNA
Ct value
EV1 2h
EV1 8h
EV1 24h
EV1 48h
Chimera 2h
Chimera 8h
Chimera 24h
Chimera 48h
CVB5 2h
CVB5 8h
CVB5 24h
CVB5 48h
Chimera cDNA

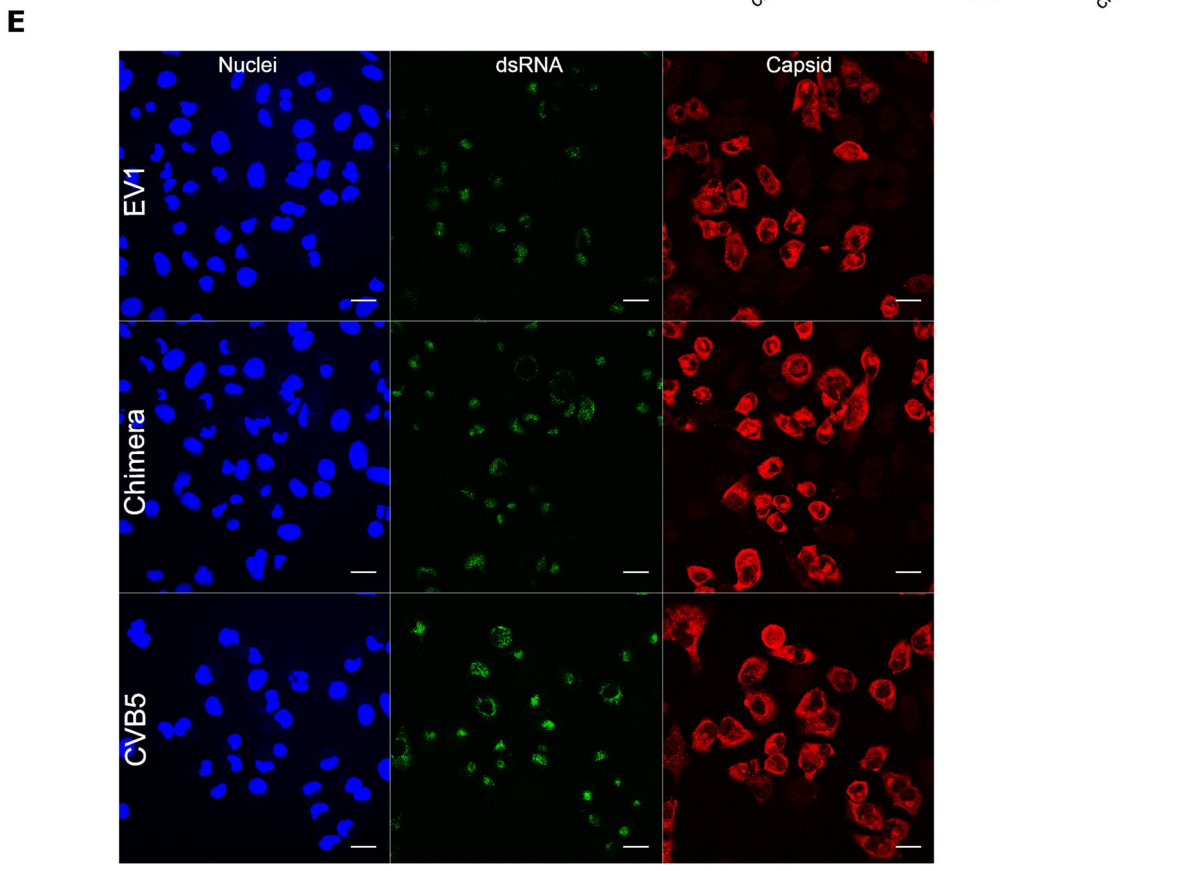
E
Nuclei
dsRNA
Capsid
EV1
Chimera
CVB5

Figure 5

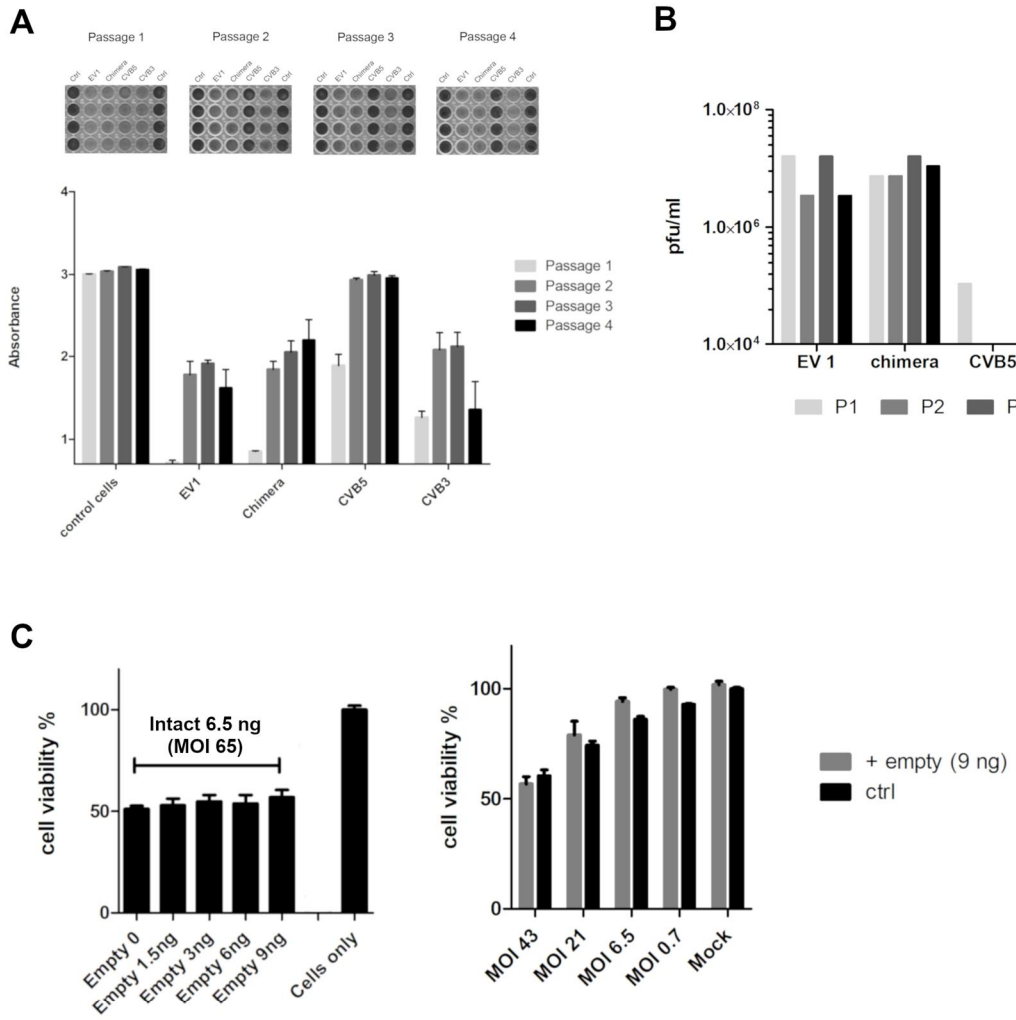
A
Passage 1
Passage 2
Passage 3
Passage 4
Absorbance
Passage 1
Passage 2
Passage 3
Passage 4
control cells
EV1
Chimera
CVB5
CVB3
B
pfu/ml
1.0×10^8
1.0×10^6
1.0×10^4
EV 1
chimera
CVB5
CVB3
P1
P2
P3
P4
C
cell viability %
Intact 6.5 ng
(MOI 65)
Empty 0
Empty 1.5ng
Empty 3ng
Empty 6ng
Empty 9ng
Cells only
cell viability %
MOI 43
MOI 21
MOI 6.5
MOI 0.7
Mock
+ empty (9 ng)
ctrl